

Efficient active transport of gene nanocarriers to the cell nucleus

Junghae Suh, Denis Wirtz, and Justin Hanes

PNAS 2003;100:3878-3882; originally published online Mar 18, 2003;
doi:10.1073/pnas.0636277100

This information is current as of March 2007.

Online Information & Services	High-resolution figures, a citation map, links to PubMed and Google Scholar, etc., can be found at: www.pnas.org/cgi/content/full/100/7/3878
Supplementary Material	Supplementary material can be found at: www.pnas.org/cgi/content/full/0636277100/DC1
References	This article cites 31 articles, 10 of which you can access for free at: www.pnas.org/cgi/content/full/100/7/3878#BIBL This article has been cited by other articles: www.pnas.org/cgi/content/full/100/7/3878#otherarticles
E-mail Alerts	Receive free email alerts when new articles cite this article - sign up in the box at the top right corner of the article or click here .
Rights & Permissions	To reproduce this article in part (figures, tables) or in entirety, see: www.pnas.org/misc/rightperm.shtml
Reprints	To order reprints, see: www.pnas.org/misc/reprints.shtml

Notes:

Efficient active transport of gene nanocarriers to the cell nucleus

Junghae Suh*, Denis Wirtz^{†*§}, and Justin Hanes^{*†§}

Departments of *Biomedical Engineering, [†]Chemical and Biomolecular Engineering, and [‡]Materials Science and Engineering, Molecular Biophysics Program, The Johns Hopkins University, 3400 North Charles Street, Baltimore, MD 21218

Edited by Robert Langer, Massachusetts Institute of Technology, Cambridge, MA, and approved February 4, 2003 (received for review October 16, 2002)

The intracellular transport of therapeutic gene carriers is poorly understood, limiting the rational design of efficient new vectors. We used live-cell real-time multiple particle tracking to quantify the intracellular transport of hundreds of individual nonviral DNA nanocarriers with 5-nm and 33-ms resolution. Unexpected parallels between several of nature's most efficient DNA viruses and nonviral polyethylenimine/DNA nanocomplexes were revealed to include motor protein-driven transport through the cytoplasm toward the nucleus on microtubules. Active gene carrier transport led to efficient perinuclear accumulation within minutes. The results provide direct evidence to dispute the common belief that the efficiency of nonviral gene carriers is dramatically reduced because of the need for their relatively slow random diffusion through the cell cytoplasm to the nucleus and, instead, focuses the attention of rational carrier design on overcoming barriers downstream of perinuclear accumulation.

Gene delivery to the cell nucleus has been implicated as the Achilles' heel of gene therapy (1). Synthetic, nonviral DNA delivery systems have been used to improve the transfer of foreign genetic material into cells, both *in vitro* (2) and *in vivo* (3). However, without evolution working to carefully hone and optimize the delivery process, manmade delivery vectors suffer from lower efficiencies compared with nature's DNA viruses. Despite this drawback, reduced immunogenicity, improved safety, and the ability to carry larger DNA loads make nonviral carriers attractive for gene therapy (4, 5). For scientists and engineers to "evolve" synthetic vectors into more efficient gene delivery vehicles, the key steps in the transfection process where viral systems show superior efficiency must first be identified.

Investigation of the intracellular trafficking of DNA carriers promises to improve the efficiency of nonviral delivery vectors by determining the rate-limiting steps of gene transfection, thereby allowing for the development of strategies to overcome these barriers (6–8). Currently, the transport of nonviral DNA carriers through the cytoplasm is poorly characterized, but is thought to be inefficient and potentially rate limiting because of their need to "randomly migrate" to the nucleus (9). Confocal microscopy has been used to study intracellular trafficking of nonviral systems (6, 10, 11), allowing the locations of complexes at discrete times to be determined, yielding an insightful but qualitative description of the transport process. Fluorescence recovery after photobleaching has recently been used to quantify overall "effective diffusion" rates of DNA molecules in the cytoplasm (12). With this ensemble-averaged technique, however, information associated with individual DNA carriers [the rates of individual particle movements, the mode of transport (e.g., random versus directed or active), and the trajectory and directionality of the transport] remains a black box.

To achieve single-particle resolution at the nanometer and 33-ms level (13, 14), we used multiple particle tracking (MPT) (13) to investigate the individual motions of hundreds of nanometer-sized nonviral DNA delivery vehicles, specifically, polyethylenimine (PEI)/DNA nanocomplexes. PEI is among the most efficient synthetic vectors for DNA delivery, a quality often attributed to its cationic nature (2), ability to protect DNA from

degradation within the cell (15), and ability to escape endosomes once the complexes are internalized (2, 16, 17). The results provide direct evidence to dispute the common belief that the efficiency of nonviral gene carriers is dramatically reduced because of the need for their relatively slow random diffusion through the cell cytoplasm to the nucleus (4, 9). In contrast, we show quantitatively that PEI/DNA nanocomplexes are efficiently transported to the perinuclear region of the cell on microtubules, leading to their rapid accumulation in that region. We also provide evidence that microtubule-based motor proteins are responsible for the transport of the nanocomplexes. Several of nature's most efficient DNA viruses exploit the same mechanisms (i.e., motor protein-ushered transport along microtubules to the perinuclear region), perhaps explaining why PEI is among the most efficient nonviral gene transfer agents known. Finally, because our studies can quantify each aspect of the intracellular transport of any fluorescently labeled moiety, including our nanocomplexes and viral particles, in real time and with high spatial and temporal resolution, they can be used to pinpoint the rate-limiting step(s) in gene delivery for any proposed carrier. The power of this quantitative approach should allow rational improvements in vector design that may ultimately result in synthetic DNA carriers with improved efficiencies.

Methods

PEI/DNA Nanocomplexes. PEI (25k branched, Sigma) fluorescently labeled with Oregon green 514 (Molecular Probes) was self-assembled with salmon DNA (Sigma) to form complexes with a nitrogen-to-phosphate ratio of 6 and an average radius of gyration of 156 ± 9 nm, as determined by time-resolved multiangle laser light scattering (TR-MALLS), and added to COS-7 cells. Methods for TR-MALLS can be found elsewhere (18). PEI and DNA solutions were in 150 mM NaCl. Complexes formed with labeled PEI and pLacZ (7.8 kb) were verified to transfect COS-7 cells (data not shown).

Cells. COS-7 cells were plated onto glass-bottom tissue culture plates (MatTek, Ashland, MA). To minimize differences caused by cell cycle stage, cells were arrested in the G₀/G₁ stage by serum deprivation (DMEM/F12 plus 10% BCS media was replaced with serum-free media). This process resulted in 80–85% of cells being in G₀/G₁ in 48 h, as determined by propidium iodide staining and fluorescence-activated cell sorter analysis (data not shown). One hour posttransfection, PEI/DNA nanocomplexes not internalized were washed away with Hank's balanced salt solution and fresh media were added.

Fluorescence Microscopy and Real-Time Particle Tracking. Cells were observed under an epifluorescence microscope (Nikon) at 37°C in the presence of 5% CO₂. At various times posttransfection, 20-s time-lapse movies were recorded with a silicon intensifier

This paper was submitted directly (Track II) to the PNAS office.

Abbreviations: MPT, multiple particle tracking; PEI, polyethylenimine; MSD, mean-square displacement.

[§]To whom correspondence may be addressed. E-mail: hanes@jhu.edu or wirtz@jhu.edu.

target camera (Dage-MTI, Michigan City, IN) at 30 frames per s. A charge-coupled device camera (Hamamatsu, Ichinocho, Japan) captured phase-contrast images. The movies were analyzed with METAMORPH software (Universal Imaging, Media, PA). Detailed methods for MPT can be found elsewhere (13, 19). Nanometer resolution was obtained on the displacements of multiple particles simultaneously by using METAMORPH to track the light-intensity-weighted centroid of diffraction-limited images, thereby achieving resolution much higher than a pixel, as reported (13, 14). Over the course of the experiment, the mean-square displacement (MSD) of 449 individual nanocomplexes within 65 cells was calculated.

Transport Mode Categorization. We calculated the effective diffusivity, $D_{\text{eff}} = \text{MSD}/(4t)$, of each gene carrier for time scales 33 ms to 10 s. If D_{eff} was constant, the carrier was categorized as diffusive. If D_{eff} decreased with time scale, the carrier was classified as subdiffusive. If D_{eff} was constant or decreased for short time scales (<1 s) and then increased at longer time scales, the gene carrier was categorized as active. The equation $\text{MSD} = 4Dt + v^2t^2$ reflects the dominance of the active transport component at longer time scales because it scales to t^2 .

Directionality of Complexes. A radius was drawn from the center of the nucleus to the position of the nanocomplex at the start and then at the end of the 20-s movie. A movement resulting in a decrease of $0.5 \mu\text{m}$ in radius was considered to be toward the nucleus, an increase of $0.5 \mu\text{m}$ was away from the nucleus, and any movement below the threshold in either direction was considered neutral. Because the $0.5\text{-}\mu\text{m}$ cutoff was arbitrary, we tested the sensitivity of our analysis with respect to choice of length scale. We found that the $0.5\text{-}\mu\text{m}$ cutoff was a good indicator of general trends found by using other arbitrary length scales up to $2 \mu\text{m}$.

Results and Discussion

The transport of nonviral gene carriers within cells was quantified and transport rates were found to be highly heterogeneous (Fig. 1A). Using MPT, the transport of individual PEI/DNA nanocomplexes was found to fall within one of three distinct subclasses (Fig. 1B): diffusive transport, subdiffusive transport, and active transport [surprisingly, a large number (up to 17%)].

Diffusive complexes [transport described by the equation $\langle \Delta r^2(t) \rangle = 4Dt$] were undergoing random, thermally driven motion in a viscous cellular medium. Here, $\langle \Delta r^2(t) \rangle$ is the MSD of the complex, D is its diffusion coefficient, and t is the time scale over which the transport is monitored. The transport rates of complexes exhibiting active transport are described by $\langle \Delta r^2(t) \rangle = 4Dt + v^2t^2$ (20) where the added term characterizes particle transport caused by directed motion, with v as the mean nanocomplex velocity. PEI/DNA nanocomplexes undergoing subdiffusive transport [described by $\langle \Delta r^2(t) \rangle \approx Kt^\alpha$, where K and α are constants, and $\alpha < 1$], may be either physically attached to an intracellular structure or contained within a viscoelastic environment, such as an endosome or a molecularly crowded region of the cytoplasm (21). With other techniques, it is not only impossible to determine the velocity of a single actively transported DNA carrier, but it is also impossible to even identify the presence of an actively transported carrier.

Complexes undergoing active transport moved several orders of magnitude faster (as measured by MSD) than complexes undergoing random thermal motion (Fig. 1B). For example, many actively transported complexes moved with velocities that would allow them to travel $10 \mu\text{m}$ in a given direction in <1 min. A PEI/DNA nanocomplex exhibiting a diffusivity of $D = 0.0008 \mu\text{m}^2/\text{s}$, the average D found from our studies, would require 8.7 h to travel $10 \mu\text{m}$ if random thermal motion was the only driving force. Most previous studies describe nonvirally delivered intra-

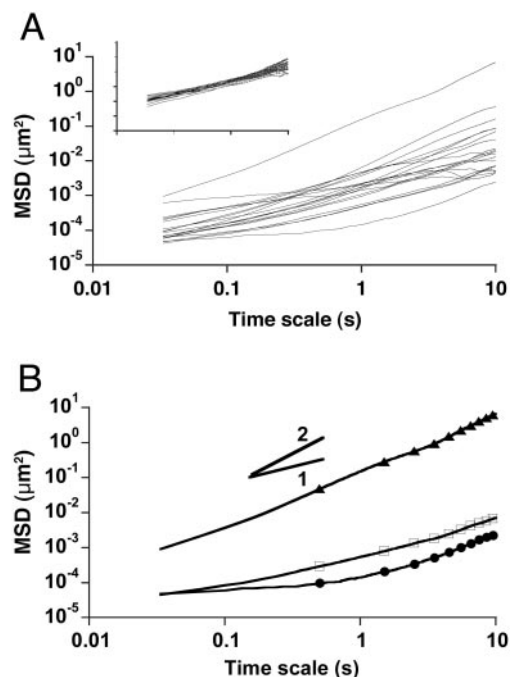


Fig. 1. Intracellular transport rates (as measured by MSD) of individual PEI/DNA nanocomplexes at 4 h posttransfection. (A) A distribution of MSD is noticeable even in this subset (20 of 60 shown) of the 4-h MSD, thus indicating the nature of the intracellular movements of complexes is highly heterogeneous. (Inset) For comparison, an example of model DNA carriers ($0.2\text{-}\mu\text{m}$ amine-modified polystyrene spheres) moving homogeneously in viscous medium (glycerol) is shown. (B) Example of MSD illustrates the three distinct transport modes. An MSD slope of 1 indicates diffusive movement (□), <1 indicates subdiffusive movement (●), and >1 indicates active transport (▲).

cellular DNA transport as purely thermal-motion driven diffusion (9, 12, 17), which underestimates the efficiency of particle transport.

The motion of actively transported PEI/DNA nanocomplexes was almost always along a path that intersected the cell nucleus, the target organelle in gene delivery (Fig. 2; Movie 1, which is published as supporting information on the PNAS web site, www.pnas.org). Microtubules within cells meet at the microtubule-organizing center located adjacent to the cell nucleus, consistent with the direction of active particle transport found in our study. MPT determined that the average velocity of actively transported complexes was $0.2 \mu\text{m}/\text{s}$, which is on the same order of magnitude as movement along microtubules involving motor proteins such as dyneins and kinesins (22). Often, actively transported PEI/DNA complexes displayed saltatory motion (Movie 1), another hallmark of motor protein-driven transport (23). Taken together, these results strongly suggest the involvement of microtubule-associated motor proteins in the active transport of PEI/DNA nanocomplexes. Actively transported complexes may be in endosomes undergoing motor protein-driven movement guided by microtubules, or they may be physically associated with the motor proteins themselves. PEI/DNA nanocomplexes may, therefore, use the same efficient mechanism for transport to the cell nucleus as several viruses, such as adenoviruses and adeno-associated viruses (24–27).

To confirm the involvement of microtubules in the active, perinuclear transport of PEI/DNA nanocomplexes, cells were treated with $10 \mu\text{M}$ nocodazole, a microtubule depolymerizing agent, for 1 h pretransfection. When examined at 2 h posttransfection, complexes in cells without microtubules displayed no directed motion (Fig. 3; Movie 2, which is published as support-

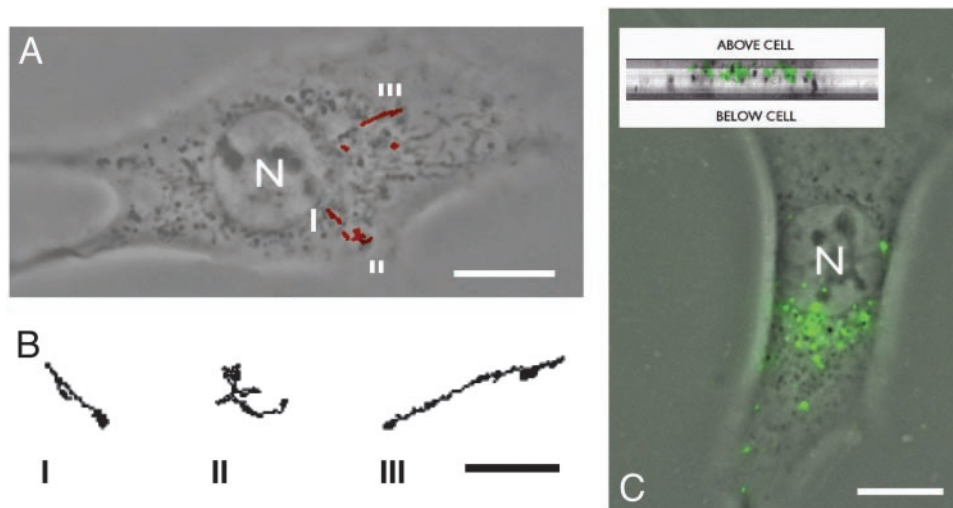


Fig. 2. Transport and locations of intracellular PEI/DNA nanocomplexes. (A) Twenty-second trajectories of PEI/DNA complexes in a COS-7 cell 4 h posttransfection. Phase-contrast image of the cell was overlaid with the trajectories of complexes. Three of six complexes shown displayed active transport with linear or curvilinear trajectories. Their detailed trajectories are shown in B. (C) COS-7 cell with PEI/DNA complexes accumulated in the perinuclear region. (Inset) Cross section of the COS-7 cell to demonstrate that PEI/DNA complexes were inside the cell. Phase-contrast image of the cell was overlaid with a fluorescent image of PEI/DNA complexes taken with the charge-coupled device camera. Some complexes appear to be intranuclear but may be within cytoplasmic invaginations that extend into the nucleus. N, nucleus. (Bars: A and C, 10 μm ; B, 2 μm .)

ing information on the PNAS web site). Additionally, the average MSD of complexes in cells without microtubules was greatly diminished (by >1 order of magnitude over a range of

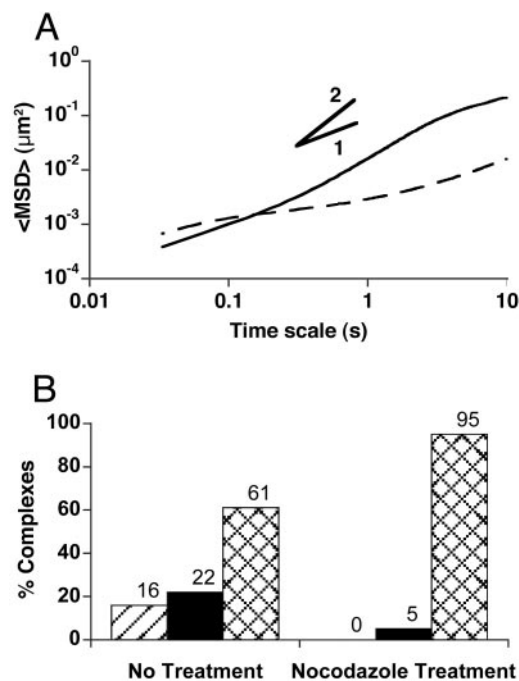


Fig. 3. Effect of microtubule depolymerization with nocodazole on the transport of PEI/DNA nanocomplexes at 2 h posttransfection. (A) The average MSD of complexes in nocodazole-treated cells (dashed line) indicates that complexes moving in cells without microtubules exhibit largely subdiffusive behavior (slope of MSD is <1) compared with complexes in cells with intact microtubules (solid line). The MSD slope of complexes in cells with intact microtubules is >1, indicating the presence of actively transported DNA carriers. (B) Nocodazole treatment abolished active motion (hatched bar) of PEI/DNA complexes. Additionally, diffusive behavior (solid bars) decreased and subdiffusive behavior (criss-cross bars) increased upon microtubule depolymerization. $n = 49$ for no nocodazole treatment case; $n = 61$ for treatment case.

time scales) compared with the cells with intact microtubules (Fig. 3A). This fourth piece of evidence further suggests that PEI/DNA nanocomplexes are ushered in a directed fashion along microtubules in a manner strikingly similar to the cytoplasmic transport of viral DNA delivery systems.

Microtubules have inherent structural polarity and motor proteins use this property to preferentially move to one end of the filament (28). Adenoviruses are known to associate with dynein (24), the motor protein that mediates movement toward the end of the microtubule that is held at the microtubule-organizing center located next to the nucleus. To determine whether PEI/DNA nanocomplexes also exploit this property, each actively transported complex was scored as to whether it moved toward, away, or neutrally relative to the nucleus center. Of the actively transported complexes tracked from 0.5 to 22.5 h posttransfection ($n = 49$), 45% moved away, 18% moved neutrally, and 37% moved toward the nucleus. Adenoviruses have been shown to preferentially move toward the microtubule-organizing center 20–40 min postinternalization (29). To our knowledge, the direction of transport of other viruses along microtubules relative to the cell nucleus has not yet been quantified, but will be a useful yardstick by which to measure the efficiency of nonviral gene carrier transport to the perinuclear region. Regardless, our result that slightly less than half of actively transported PEI/DNA nanocomplexes were carried preferentially toward the nucleus after the first 30 min of transfection suggests there exists room for improvement in the efficiency of these carriers for gene therapy applications.

Despite the lack of preferential movement toward the nucleus by actively transported particles after the first 30 min of transfection, PEI/DNA nanocomplexes were observed to rapidly accumulate in the perinuclear region (Fig. 2C). To study the intracellular spatial variation of DNA carrier transport, the cytoplasm of each cell was divided into four quadrants (Q1–Q4, Fig. 4A). Surprisingly, an average of 41% of total PEI/DNA nanocomplexes was found in the perinuclear quadrant Q1 within 30 min of posttransfection. The other three quadrants each contained 20% of the complexes. The percentage of complexes in Q1 was statistically significant ($P < 0.005$) compared with the other quadrants. Accumulation in the perinuclear region within

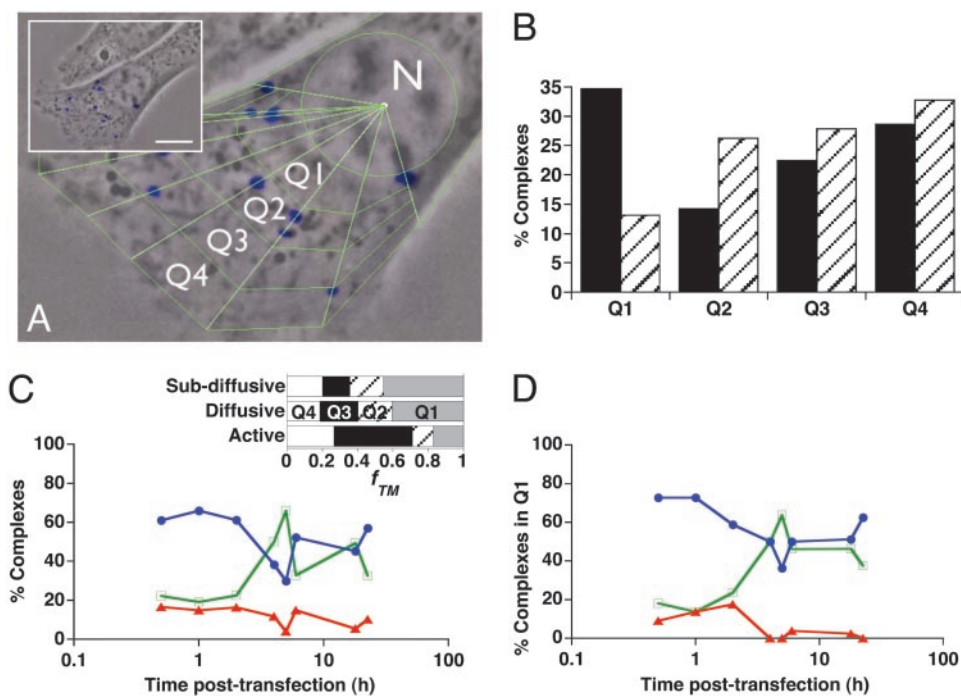


Fig. 4. Intracellular transport of PEI/DNA complexes depends on spatial location and time posttransfection. (A) To determine cytoplasmic locations of complexes, a radius was drawn connecting the nucleus center, the complex, and the plasma membrane. With the nuclear envelope and plasma membrane as boundaries, the radius was divided into four equal segments to yield the borders of four quadrants (Q1–Q4). N indicates nucleus. (Inset) The cell without quadrants and with complexes in blue. (Bar: 10 μm .) (B) Locations of complexes at 2 h posttransfection in cells with intact microtubules (black columns) and in nocodazole-treated cells (hatched columns). Note the lack of perinuclear accumulation in cells without intact microtubules. (C) Transport modes of all intracellular complexes over 22.5 h posttransfection were divided into diffusive (\square), subdiffusive (\bullet), and active transport (\blacktriangle). Actively transported complexes had velocities of $0.1 \leq v \leq 0.49 \mu\text{m}/\text{s}$. Diffusive complexes had diffusivities between 0.0001 and $0.0065 \mu\text{m}^2/\text{s}$, with an average of $0.0008 \mu\text{m}^2/\text{s}$. Subdiffusive complexes displayed a characteristic exponent, α , ranging from 0.2 to 0.9. The percentage of diffusive complexes increased over time, whereas the proportion of subdiffusive complexes decreased. The 4-h mark stands out as the first time the percentage of diffusive complexes exceeded that of subdiffusive. Complexes divided into the three transport modes were further assigned to the four quadrants (Inset). f_{TM} represents the fraction of complexes of a specific transport mode. When averaged over all times posttransfection, Q1 held the largest fraction of diffusive ($f_{\text{TM}} = 0.41$) and subdiffusive ($f_{\text{TM}} = 0.45$) complexes, and Q3 contained the most actively transported complexes ($f_{\text{TM}} = 0.45$). These values were statistically significant ($P < 0.005$) compared with other quadrants within each transport mode. (D) Transport modes of complexes in the perinuclear region (Q1) were categorized as in C.

30 min is another unexpected parallel between gene delivery with adenoviruses or adeno-associated viruses (24, 25) and PEI/DNA complexes. Perinuclear accumulation of PEI gene carriers has been reported to require at least 1 h (6, 10). Potential explanations for the discrepancy include differences in cell type (COS-7 in our studies versus L929 or EA.hy926), cell cycle stage (our cells were nondividing), and gene carrier preparation parameters (e.g., the nitrogen-to-phosphate ratio is 6 in our studies versus a nitrogen-to-phosphate ratio of 10 or 7.5). Differences in carrier preparation can lead to changes in complex size, surface charge, and/or density. Interestingly, no such accumulation of PEI/DNA nanocomplexes was observed within cells treated with nocodazole (i.e., cells without microtubules, Fig. 4B, Movie 2), evidence that microtubule-assisted active transport is responsible for the perinuclear accumulation of PEI/DNA complexes. Note that we observed significant perinuclear accumulation within 30 min, but did not observe preferential movement of actively transported carriers toward the nucleus after the first 30 min of transfection. Q1 contained $\approx 40\%$ of internal PEI/DNA complexes at all time points after 30 min. One implication is that preferential active transport to the nuclear region occurs within the first 30 min posttransfection. This period of preferential active transport to the nucleus is similar to that seen with adenoviruses (29).

An important implication of these results is that reaching the nucleus is not a rate-limiting step for PEI/DNA complex-mediated gene transfection in COS-7 cells. The search for the

rate-limiting step in gene delivery and transfection with PEI/DNA complexes (at least in COS-7 cells) must consider possibilities other than inefficient transport to the perinuclear region, such as endosomal escape (30–32), nuclear import (8), and vector unpacking (5).

Adenoviruses are known to escape endosomes and subsequently travel along microtubules to the nucleus in a directed fashion (24). Adeno-associated viruses, on the other hand, are thought to reach the perinuclear region within endosomes (that are actively transported on microtubules) and then break free of the vesicles before entering the nucleus (25–27). Like adeno-associated viruses, PEI/DNA complexes likely accumulate in the perinuclear region within endosomes (10). Complexes inside quasi-stationary endosomes, located in the perinuclear region, may exhibit subdiffusive behavior caused by the confining cage-like nature of endosomal compartments. Therefore, as PEI/DNA nanocomplexes escape their endosomal cage into the cytosol, the percentage of complexes exhibiting subdiffusive behavior was expected to decrease. As expected, the proportion of subdiffusive complexes in the perinuclear region (region Q1) decreased from 73% at 0.5 h to 50% at 4 h, during which time the percentage of diffusive complexes increased from 18% to 50% (Fig. 4D). These trends were somewhat reiterated in Q2, but not in Q3 or Q4 (data not shown). Thus, a clear transition from subdiffusive to diffusive behavior of PEI/DNA nanocomplexes occurred in areas closest to the nucleus between 1 and 4 h posttransfection. This transition may be caused by PEI/DNA

escape from their endosomal carriers. An alternative explanation could be that endosomes themselves dissociate from microtubules in the perinuclear region and begin to diffuse randomly. A previous study also highlighted this approximate time frame as a temporal landmark in the transfection process, showing PEI/DNA complexes enter the cell nucleus by 4.5 h posttransfection (6). Complexes were not found to enter the nucleus in our studies, which may be because of differences in cell type, cell cycle stage, and PEI/DNA nanocomplex parameters. Differences in cell cycle stage between our study (nondividing cells) and that by Godbey *et al.* (ref. 6, mitotic cells) may be the most likely reason for this difference. Channels created by nuclear pore complexes can be expanded to a maximum size of ≈ 30 nm (33); therefore, the vast majority of PEI gene carriers are too large to pass into the nucleus of nondividing cells. In mitotic cells, however, the nuclear membrane breaks down temporarily, potentially allowing gene carriers access to the nuclear space.

Cationic particles, such as PEI/DNA nanocomplexes, that escaped endosomes are not expected to remain diffusive indefinitely because of electrostatic or other attractions to quasi-stationary intracellular components, potentially including the nucleus. Therefore, a transition from diffusive back to subdiffusive transport is expected over longer times in the perinuclear region. Indeed, PEI/DNA nanocomplexes show such a shift at times >4 h (Fig. 4C).

Uptake by endocytosis, motor protein-driven directed motion through the cytoplasm on microtubules, escape from endosomes, and rapid perinuclear accumulation are steps in the transfection

process shared by efficient viral DNA carriers and nonviral PEI/DNA complexes. These common traits focus our attention on efficiency of endosomal escape, nuclear entry, and vector unpacking as possible rate-limiting steps in PEI-mediated gene transfection of COS-7 cells.

The analysis presented here complements existing techniques to study intracellular transport, including fluorescence recovery after photobleaching (12) and confocal microscopy (6). Our results offer quantitative insights into the intracellular transport mechanisms of PEI/DNA complexes. With MPT, we showed that gene carrier transport within cells was highly dynamic, displaying remarkable temporal and spatial variations. The ability to accurately measure such variations may, in the future, be useful in the temporal and spatial pinpointing of intracellular phenomena with high relevance to intracellular drug delivery and gene therapy. Current investigations using MPT focus on a quantitative comparison of the transfection processes, in real time, of viral and nonviral DNA carriers in various cell types. The goal of these studies is to elucidate the critical barriers to gene delivery and further shape the paradigm of successful nonviral DNA vector design.

We thank John van Zanten and Yah-el Har-el for assistance with PEI/DNA complex characterization by time-resolved multiangle laser light scattering, Eric Krauland for insightful discussions, and Thomas Kole, Yiider Tseng, and Jerry Lee for technical assistance. This work was supported by Whitaker Foundation Grant RG-99-0046, National Institutes of Health Grant T32-GM07057, and National Science Foundation Grant CTS0210718.

- Verma, I. M. & Somia, N. (1997) *Nature* **389**, 239–242.
- Boussif, O., Lezoualc'h, F., Zanta, M. A., Mergny, M. D., Scherman, D., Demeneix, B. & Behr, J. P. (1995) *Proc. Natl. Acad. Sci. USA* **92**, 7297–7301.
- Gautam, A., Densmore, C. L., Golunski, E., Xu, B. & Waldrep, J. C. (2001) *Mol. Ther.* **3**, 551–556.
- Luo, D. & Saltzman, W. M. (2000) *Nat. Biotechnol.* **18**, 33–37.
- Schaffer, D. V., Fidelman, N. A., Dan, N. & Lauffenburger, D. A. (2000) *Biotechnol. Bioeng.* **67**, 598–606.
- Godbey, W. T., Wu, K. K. & Mikos, A. G. (1999) *Proc. Natl. Acad. Sci. USA* **96**, 5177–5181.
- Varga, C. M., Hong, K. & Lauffenburger, D. A. (2001) *Mol. Ther.* **4**, 438–446.
- Wolff, J. A. & Sebestyen, M. G. (2001) *Nat. Biotechnol.* **19**, 1118–1120.
- Kircheis, R., Wightman, L. & Wagner, E. (2001) *Adv. Drug Delivery Rev.* **53**, 341–358.
- Remy-Kristensen, A., Clamme, J. P., Vuilleumier, C., Kuhry, J. G. & Mely, Y. (2001) *Biochim. Biophys. Acta* **1514**, 21–32.
- Ishii, T., Okahata, Y. & Sato, T. (2001) *Biochim. Biophys. Acta* **1514**, 51–64.
- Lukacs, G. L., Haggie, P., Seksek, O., Lechardeur, D., Freedman, N. & Verkman, A. S. (2000) *J. Biol. Chem.* **275**, 1625–1629.
- Apgar, J., Tseng, Y., Fedorov, E., Herwig, M. B., Almo, S. C. & Wirtz, D. (2000) *Biophys. J.* **79**, 1095–1106.
- Crocker, J. C. & Grier, D. G. U. (1996) *J. Colloid Interface Sci.* **179**, 298–310.
- Godbey, W. T., Barry, M. A., Saggau, P., Wu, K. K. & Mikos, A. G. (2000) *J. Biomed. Mater. Res.* **51**, 321–328.
- Klemm, A. R., Young, D. & Lloyd, J. B. (1998) *Biochem. Pharmacol.* **56**, 41–46.
- Kichler, A., Leborgne, C., Coeytaux, E. & Danos, O. (2001) *J. Gene Med.* **3**, 135–144.
- Lai, E. & van Zanten, J. H. (2001) *Biophys. J.* **80**, 864–873.
- Tseng, Y. & Wirtz, D. (2001) *Biophys. J.* **81**, 1643–1656.
- Qian, H., Sheetz, M. P. & Elson, E. L. (1991) *Biophys. J.* **60**, 910–921.
- Yamada, S., Wirtz, D. & Kuo, S. C. (2000) *Biophys. J.* **78**, 1736–1747.
- King, S. J. & Schroer, T. A. (2000) *Nat. Cell Biol.* **2**, 20–24.
- Rietdorf, J., Ploubidou, A., Reckmann, I., Holmstrom, A., Frischknecht, F., Zettl, M., Zimmermann, T. & Way, M. (2001) *Nat. Cell Biol.* **3**, 992–1000.
- Leopold, P. L., Kreitzer, G., Miyazawa, N., Rempel, S., Pfister, K. K., Rodriguez-Boulan, E. & Crystal, R. G. (2000) *Hum. Gene Ther.* **11**, 151–165.
- Bartlett, J. S., Wilcher, R. & Samulski, R. J. (2000) *J. Virol.* **74**, 2777–2785.
- Seisenberger, G., Ried, M. U., Endress, T., Buning, H., Hallek, M. & Brauchle, C. (2001) *Science* **294**, 1929–1932.
- Douar, A. M., Poulard, K., Stockholm, D. & Danos, O. (2001) *J. Virol.* **75**, 1824–1833.
- Lodish, H., Berk, A., Zipursky, S. L., Matsudaira, P., Baltimore, D. & Darnell, J. (2000) *Molecular Cell Biology* (Freeman, New York).
- Suomalainen, M., Nakano, M. Y., Keller, S., Boucke, K., Stidwill, R. P. & Greber, U. F. (1999) *J. Cell Biol.* **144**, 657–672.
- Plank, C., Oberhauser, B., Mechtler, K., Koch, C. & Wagner, E. (1994) *J. Biol. Chem.* **269**, 12918–12924.
- Pack, D. W., Putnam, D. & Langer, R. (2000) *Biotechnol. Bioeng.* **67**, 217–223.
- Ogris, M., Carlisle, R. C., Bettinger, T. & Seymour, L. W. (2001) *J. Biol. Chem.* **276**, 47550–47555.
- Nigg, E. A. (1997) *Nature* **386**, 779–787.